Available online at www.sciencedirect.com
SCIENCE DIRECT
Journal of Power Sources 158 (2006) 806–814
JOURNAL OF POWER SOURCES
www.elsevier.com/locate/jpowsour

Control strategy of fuel cell/supercapacitors hybrid power sources for electric vehicle

Phatiphat Thounthong *, Stéphane Raël, Bernard Davat

Institut National Polytechnique de Lorraine (INPL), GREEN, CNRS (UMR 7037) 2, Avenue de la Forêt de Haye, 54516 Vandœuvre-lès-Nancy, France

Received 15 May 2005; accepted 6 September 2005
Available online 22 November 2005

Abstract

This paper presents a control principle for utilizing PEM fuel cell as main power source and supercapacitors as auxiliary power source for electric vehicle applications. The strategy is based on dc link voltage regulation, and fuel cell is simply operating in almost steady state conditions in order to minimize the mechanical stresses of fuel cell and to ensure a good synchronization between fuel flow and fuel cell current. Supercapacitors are functioning during transient energy delivery or transient energy recovery. To authenticate control algorithms, the system structure is realized by analogical current loops and digital voltage loops (dSPACE). The experimental results with a 500 W PEM fuel cell point out the fuel cell starvation problem when operating with dynamic load, and also confirm that the supercapacitor can improve system performance for hybrid power sources.

Keywords: Electric vehicle; Hybrid electrical system; Polymer electrolyte membrane fuel cell; Power electronics; Supercapacitor

1. Introduction

In this day and age, fuel cell (FC) power generation systems are expected to be used in more and more applications. For portable power, a fuel cell coupled with a fuel container can offer a higher energy storage density and more convenience than conventional battery systems [1]. In transportation applications, fuel cells offer higher efficiency than conventional engines coupled with electrical generators, but the main task is still to develop a cost-effective, reliable and safe method of storing sufficient hydrogen on-board the vehicle [2]. In stationary power applications, low emissions permit fuel cells to be located in high power density areas where they can supplement the existing electrical network. Furthermore, fuel cell systems can be directly connected to a building to provide both power and heat with higher overall efficiencies [3].

There are several types of fuel cells, which are characterized by the employed electrolyte. The chemical makeup of each type determines its operating characteristics. Scientists are developing many different types of fuel cells employing different fuels and electrolytes. One of the most promising for electric vehicles is the lightweight, relatively easy to build and small polymer electrolyte membrane fuel cell (PEMFC) [4].

Different previous works have already pointed out the possibility to use fuel cell in distributed power generation systems. Chandler et al. [5] reported experimental results carried out on a Fuel Cell Transit Bus, known as hybrid fuel cell/battery bus prepared for the U.S. Department of Energy (DOE). This bus has a rated power of 60 kW, and its energy source is composed of a UTC PEM fuel cell (60 kW, 160–250 V) as main power source, and of 48 Panasonic lead-acid 12-V batteries associated in series as auxiliary source. In addition, Rodatz et al. [6] presented the field tests, in urban and highway sections, of a Fuel Cell/Supercapacitor-Powered Hybrid Vehicle with a PEM fuel cell (40 kW, 150 A), a supercapacitor module (5.67 F, 250 A, 360 V), and an ac motor (45 kW). This work also explained one of the key week points of fuel cell, which is dynamic limitation. In fact, fuel cell voltage is highest when no current is flowing, and drops with increasing current because of activation overvoltage and ohmic resistance losses in the membrane. At high currents, the voltage drops sharply as the transport of reactant gases is not able to follow the amount used in the reaction. Consequently, reactant starvation occurs at the reaction side and the cell fails. Since a current is drawn through the stack, the failed cell may start to operate as an electrolytic cell and cause

* Corresponding author. Tel.: +33 383 59 56 54; fax: +33 383 59 56 53.
E-mail address: Phatiphat.Thounthong@ensem.inpl-nancy.fr (P. Thounthong).

0378-7753/$ – see front matter © 2005 Elsevier B.V. All rights reserved.
doi:10.1016/j.jpowsour.2005.09.014

irreversible damage. Therefore, the current that can be supplied by the fuel cell needs to be limited. Moreover, a lag between fuel cell load current and response of the reactant supply system results in an undersupply of reactants to the fuel cell. This leads to a breakdown of the chemical reaction and to a rapid loss in voltage. This phenomenon may be avoided by restricting the dynamics of the load. Therefore, in P. Rodatz's tests, the dynamic of the fuel cell system was limited to a conservative 2.5 kW s^{-1}.

Pukrushpan et al. [7,8], furthermore, attempted to improve fuel cell dynamics by controlling fuel cell processor in order to avoid fuel starvation, when current is rapidly drawn from fuel cell. In addition, Schenck et al. [9], working with a Ballard Nexa™ PEM fuel cell (1.2 kW), and Thounthong et al. [10], working with a ZSW PEM fuel cell (0.5 kW), evidently demonstrated the fuel cell starvation phenomenon when fuel cell worked with step electrical loads. They demonstrated that its dynamics was limited by the hydrogen and oxygen delivery system, which contains pumps, valves, and in some cases, a hydrogen reformer. They recommended to utilize fuel cell, as main power source, with at least a fast auxiliary power source to improve the system performances. Additionally, fuel cell has slow dynamics by nature. If it is operated in nearly steady state condition in order to circumvent fast change of fuel cell current, mechanical stresses are avoided, and lifetime of fuel cell stack will increase [11].

Besides, in electrical network of electric vehicle, the dc bus voltage control has problem when electrical loads demand or recover high energy in short time (for example, while wheel motors start or brake). Consequently, in order to answer these problems, the system must have a rapid supplementary power source to deliver or to absorb high transient energy. Choi et al. [12] and Burke [13] reported that the innovative high current supercapacitor technology has been developed for this reason. Then, the very fast power response of supercapacitors can be used to match the slower power output of the fuel cell to produce the compatibility and performance characteristics needed by distributed system.

Precisely, Rufer et al. [14] already proposed a solution by utilizing a supercapacitive-storage-based substation with 60 V, 200 A, 75 F supercapacitor tank (series association of 24 supercapacitors 1800 F) for the compensation of resistive voltage drops in transportation networks. Dixon et al. [15] also presented a hybrid battery/supercapacitor vehicle with a 32 kW wheel motor, and a supercapacitor bank (300 V, 200 A, 20 F). J. W. Dixon's work was designed and implemented to manage power flow between a supercapacitor bank and lead-acid batteries. Supercapacitors are controlled for higher accelerations and decelerations of the vehicle with minimal loss of energy, and minimal degradation of the main battery pack.

This paper presents a small-scale test bench of 42 V, 500 W dc bus having a PEM fuel cell as main source and supercapacitors as auxiliary source as proposed in Fig. 1 [16]. It especially details a new control strategy based on a sharing of energy between the two sources taking into account the low dynamics of the fuel cell. The experimental results are divided in two parts. The first one shows only PEM fuel cell characteristics when connecting with converter to the dc bus, and the second one shows hybrid source characteristics for different situations while connecting to dc bus in order to confirm system operation.

2. Hybrid power sources

In general, dc bus voltage v_{Bus} (for example, 500 V for Toyota Prius Hybrid Vehicle) is higher than fuel cell voltage v_{FC}. As a result, fuel cell converter, which delivers a directional current, has to boost the fuel cell voltage to the dc bus level. Supercapacitor converter controls a bidirectional current in order to store or generate energy as presented in Fig. 1. The studied hybrid source comprises a small-scale 42 V dc bus supplied by a 500 W PEM fuel cell and a supercapacitive storage device. The function of the fuel cell is to supply mean power to the load, whereas the storage device is used as a power source: it supplies transient power demand, and peak loads required during acceleration and deceleration.

2.1. Fuel cell converter [10]

Fuel cell operates giving direct current at a low voltage; thereby, the boost converter, presented in Fig. 2, is selected to adapt the low dc voltage delivered by the fuel cell, which is around 12.5 V at its rated power, to the 42 V dc bus. The fuel cell converter, designed for a 25 kHz PWM is composed of a high frequency inductor L_1, a total dc bus capacitor C, a diode D_1 (STPS80H100TV: 100 V, 40 A) and a main switch S_1. Switch S_2 is a shutdown device for test security to prevent the fuel cell stack from short circuits in case of accidental destruction of S_1,

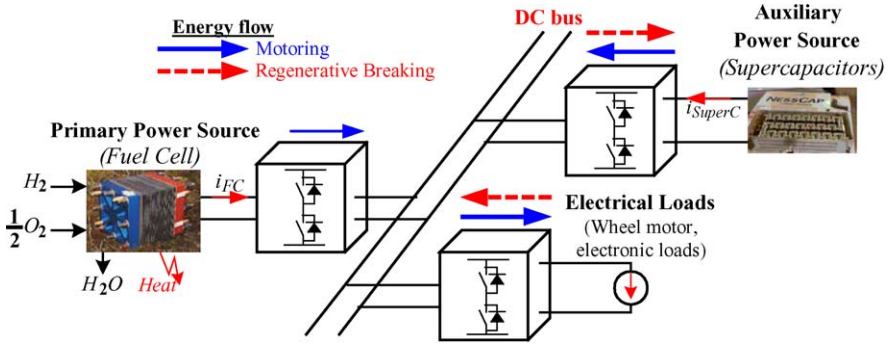

Fig. 1. Fuel cell/supercapacitor hybrid power sources.

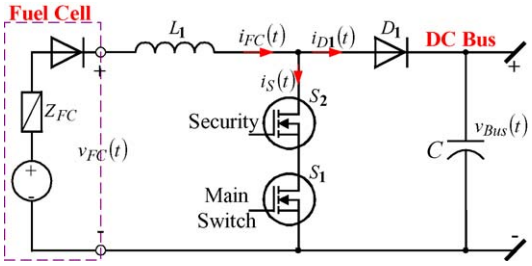

Fig. 2. Fuel cell boost converter.

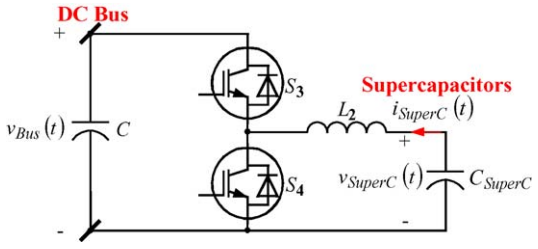

Fig. 3. 2-quadrant supercapacitor converter.

or faulty operation of the regulator. S_1 and S_2 are STE180NE10 (100 V, 180 A).

The fuel cell converter is driven, through MOSFET S_1 gate signal, by means of a pulse width modulation (PWM) for average current control, in order to obtain constant switching frequency for fuel cell current. The used PWM generator is a high-speed PWM generator UC28025B (Texas Instruments Inc.). The special features of this generator are suitability for average current control, soft start and pulse-by-pulse current limitation.

2.2. Supercapacitor converter

The supercapacitors are connected to the dc bus by means of a 2-quadrant dc/dc converter, as shown in Fig. 3. L_2 represents the inductor used for energy transfer and filtering. The inductor size is classically defined by switching frequency and current ripple [17]. Rufer et al. [18] already presented that supercapacitor size is defined by dc bus energy requirements deduced from hybrid power profile. The supercapacitor current, which flows across the storage device, can be positive or negative, allowing energy to be transferred in both directions. Finally, the converter is driven by means of complementary pulses, generated by a hysteresis comparator, and applied on the gates of the two MOSFET S_3 and S_4 (in one module SKM200 GB 123D: 200 A, 1200 V).

2.3. Hybrid control structure

The proposed hybrid control is depicted in Fig. 4. For reasons of safety and dynamics, the fuel cell and supercapacitor converters are primary operated by inner current loop controls which are realized by analogical circuits. Therefore, current commands of fuel cell and supercapacitors depend on conditions of hybrid operation. Moreover, classical PID controller is selected for "Fuel Cell Current Controller", which generates duty ratio signal for the PWM generator. A hysteresis controller is selected for "Supercapacitor Current Controller".

Because fuel cell is supplied with gas through pumps, valves and compressors, it has large time constants (several seconds). As a result, it cannot accurately reply to fast increasing or decreasing power loads, and may be damaged by repetitive stepped power loads. For this reason, the fuel cell in the hybrid system is only operating in nearly steady state conditions, and supercapacitors are functioning during transient energy delivery or transient energy recovery.

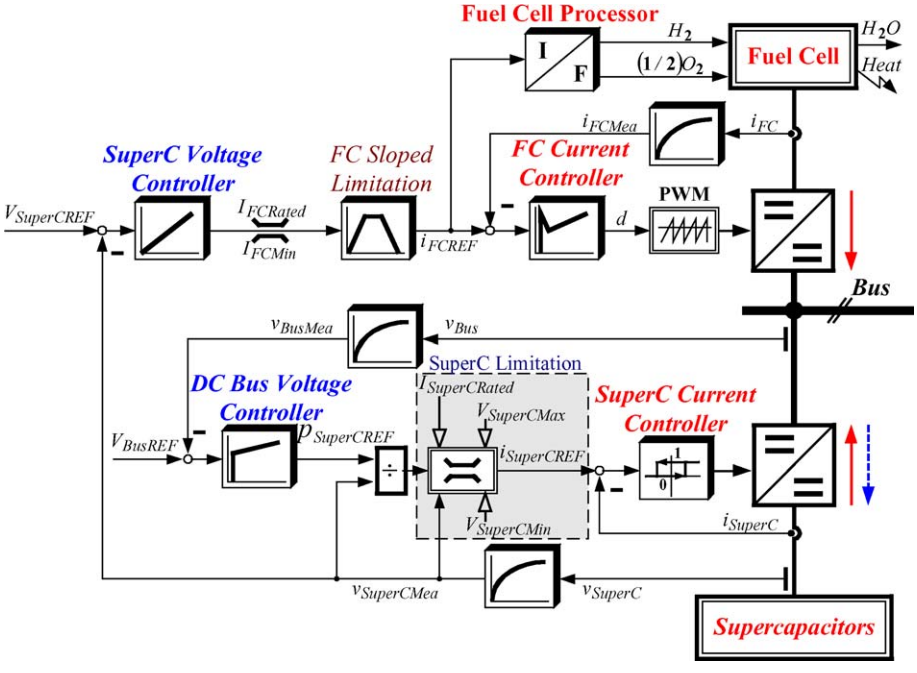

Fig. 4. Proposed hybrid system control structure.

The main objective of the control is to regulate dc bus voltage v_{Bus}. Taking into account of fuel cell dynamics, hybrid control system generates two current reference signals i_{FCREF} for fuel cell and $i_{SuperCREF}$ for supercapacitors with the following constraints:

(1) Fuel cell current slope must be limited to a maximum absolute value (for example, 4 A s^{-1} [19]) in order to guarantee matching the reactant delivery rate and the usage rate.
(2) Fuel cell current must be kept within an interval [$I_{FCRated}$ (rated value), I_{FCMin} (minimum value) or zero].
(3) Supercapacitive storage device voltage must be kept within an interval [$V_{SuperCMin}$ (minimum value), $V_{SuperCMax}$ (maximum value)]. Normally, the system attempts to reach the normal voltage $V_{SuperCNormal}$.

Note that fuel cell current reference i_{FCREF} is synchronously sent to fuel cell processor, in order to adjust hydrogen and oxygen flows to the desired electrical current.

In previous work, Rufer et al. [14] already proposed to employ supercapacitors-based substation for compensating voltage drop on a 700 V dc bus in which the control of supercapacitor converter is independent from dc main source rectifier. With a fuel cell as main source, Thounthong et al. [20] have tried in hybrid sources built with a PEM fuel cell as main source and supercapacitors as secondary source to regulate the dc bus voltage through a power control (*load power = fuel cell power + supercapacitor power*), with a limitation of the fuel cell current slope. One of the major problems, which appear in such a control, is the presence of mode definitions (motoring or generative braking, for example) with difficulties to avoid instability when operating at the border of two different modes.

For this reason, the novel conception is that the hybrid system control proposes a regulation of the dc bus voltage through the power only delivered by the fast auxiliary source, here the supercapacitors. And supercapacitor voltage is regulated to $V_{SuperCNormal}$ through the slow main source, the fuel cell.

More precisely, the "dc bus voltage controller" (PI controller) generates a power reference, called $p_{SuperCREF}$. By power law conservation and no loss assumption, the supercapacitor current reference is a consequence of the power demand. It is calculated by dividing the power reference $p_{SuperCREF}$ by the measured supercapacitor voltage. Because this voltage contains harmonics due to the converter switching and the series resistance of device (ESR), the measured signal must be filtered by low pass filter with low cut-off frequency (for instance, 1 Hz).

Besides, the supercapacitor voltage controller (I controller) generates a fuel cell current reference i_{FCREF}. This signal is limited in level ($I_{FCRated}$ and I_{FCMin}) and in slope, the first and second constraints. By this strategy, system can visibly guarantee that fuel cell current will gradually increase and decrease, and over rated or lower minimum fuel cell current will not happen. Note that minimum value for fuel cell current is set in order to maintain continuous conducting mode of fuel cell current. Fuel cell current, in addition, is functioned at slow dynamics, and in this case, integral controller (I controller) is enough for supercapacitor voltage controller, and it also ensures no static error.

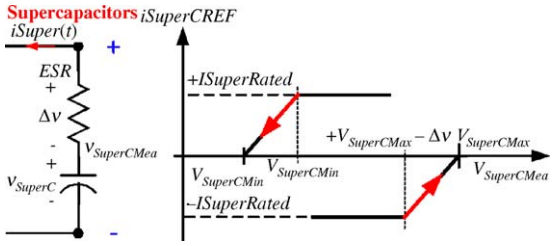

Fig. 5. Supercapacitors current limitation functions.

Finally, to keep the supercapacitor voltage within its defined limit [$V_{SuperCMin}$, $V_{SuperCMax}$], the last constraint, the supercapacitor current has to be limited. For example, during regenerative breaking, fuel cell current is limited at its minimum value. As a consequence, the dc bus voltage will exceed its reference value, and hence the voltage controller will reduce power reference to a negative value. It means that over energy will be stored in supercapacitors, and supercapacitor voltage will increase over $V_{SuperCNormal}$. While charging, system must limit supercapacitor voltage to $V_{SuperCMax}$. Hybrid system, for this reason, ensures supercapacitor voltage limitation by limiting current as proposed in Fig. 5.

The minimum negative current during charging can be revealed by:

$$I_{SuperCMin} = -I_{SuperCRated} \times \min\left(1, \frac{v_{SuperCMax} - v_{SuperCMea}}{\Delta v}\right) \quad (1)$$

For example, with $V_{SuperCNormal}$ ($V_{SuperCREF}$) = 13 V, $V_{SuperCMax}$ = 15 V, $I_{SuperCRated}$ = 200 A, and Δv = 0.5 V (which corresponds to an average value of the voltage drop across the ESR fixed once for the considered work), if $v_{SuperCMea}$ = 14 V, one obtains $I_{SuperCMin} = -200$ A. In this case, where supercapacitor voltage is far from $V_{SuperCMax}$, the charging current limit $I_{SuperCMin}$ is equal to its negative rated value $-I_{SuperCRated}$. In the case, when the supercapacitor voltage is closed to its maximum limit, the charging current limit $I_{SuperCMin}$ becomes greater than its negative rated value $-I_{SuperCRated}$. For instance, when $v_{SuperCMea}$ is equal to 14.8 V, the charging current limit becomes −80 A.

With the same principle, one defines the upper boundary of the discharging supercapacitor current as:

$$I_{SuperCMax} = I_{SuperCRated} \times \min\left(1, \frac{v_{SuperCMea} - v_{SuperCMin}}{\Delta v}\right) \quad (2)$$

3. System equations

3.1. Fuel cell current loop

To obtain the transfer function of the fuel cell current loop, the linearized differential equations are defined as follows

[21,22]:

$$L_1\frac{\mathrm{d}\tilde{i}_{\mathrm{FC}}(t)}{\mathrm{d}t} = \tilde{v}_{\mathrm{FC}}(t) - R_{L_1}\tilde{i}_{\mathrm{FC}}(t) - (1-D)\tilde{v}_{\mathrm{Bus}}(t) + V_{\mathrm{Bus}}\tilde{d}(t) \tag{3}$$

$$C\frac{\mathrm{d}\tilde{v}_{\mathrm{Bus}}}{\mathrm{d}t} = (1-D)\tilde{i}_{\mathrm{FC}} - I_{\mathrm{FC}}\tilde{d} - \tilde{i}_{\mathrm{load}} \tag{4}$$

where D is the nominal duty ratio of the PWM fuel cell converter, $\tilde{d}$ is the duty ratio variation, V_{Bus} is the nominal dc bus voltage, $\tilde{v}_{\mathrm{Bus}}$ is the dc bus voltage variation, I_{FC} is the nominal fuel cell current, $\tilde{i}_{\mathrm{FC}}$ is the fuel cell current variation, $\tilde{i}_{\mathrm{load}}$ is the load current variation and R_{L_1} is the series resistance of L_1. Note that series resistance of C is ignored.

From (3) and (4), the fuel cell current loop can be modeled by the following transfer function:

$$\left.\frac{\tilde{i}_{\mathrm{FC_{Mea}}}(s)}{\tilde{i}_{\mathrm{FC_{REF}}}(s)}\right|_{\mathrm{OL}} = \overbrace{G_C\frac{(T_{\mathrm{Ci}}s+1)}{T_{\mathrm{Ci}}s}\frac{(T_{\mathrm{Cd}}s+1)}{(T'_{\mathrm{cd}}s+1)}}^{\text{PID Controller}} \times \overbrace{\frac{1}{V_{\mathrm{P}}}}^{\text{PWM}} \times \overbrace{\frac{G_i(T_z s+1)}{(s/\omega_n)^2+(2\zeta/\omega_n)s+1}}^{\tilde{i}_{\mathrm{FC}}(s)/\tilde{d}(s)} \times \overbrace{\frac{K_1}{T_{\mathrm{fc}}s+1}}^{\text{filter}} \tag{5}$$

where V_{P} is the amplitude of the PWM saw tooth carrier signal, and

$$\left.\begin{aligned} G_i &= \frac{I_{\mathrm{FC}}}{(1-D)}, & T_z &= \frac{V_{\mathrm{Bus}}C}{(1-D)I_{\mathrm{FC}}} \\ \omega_n &= \sqrt{\frac{(1-D)^2}{L_1 C}}, & \zeta &= \frac{R_{L_1}C}{(1-D)^2}\frac{\omega_n}{2} \end{aligned}\right\} \tag{6}$$

3.2. DC bus voltage loop

To obtain the transfer function of the dc bus voltage loop, one can write power conservation equation with the assumption that system has no losses:

$$p_{\mathrm{SuperC}}(t) = Cv_{\mathrm{Bus}}(t)\frac{\mathrm{d}v_{\mathrm{Bus}}(t)}{\mathrm{d}t} + v_{\mathrm{Bus}}(t)i_{\mathrm{load}}(t) \tag{7}$$

where p_{SuperC} is the power supplied by supercapacitors, i_{load} is the load current, which can be considered as a disturbance of the system.

The linearized differential equation can be written as follows:

$$\tilde{p}_{\mathrm{SuperC}} = CV_{\mathrm{Bus}}\frac{\mathrm{d}\tilde{v}_{\mathrm{Bus}}}{\mathrm{d}t} + I_{\mathrm{load}}\tilde{v}_{\mathrm{Bus}} + V_{\mathrm{Bus}}\tilde{i}_{\mathrm{load}} \tag{8}$$

where $\tilde{p}_{\mathrm{SuperC}}$ is the variation of power supplied by supercapacitors, I_{load} is the nominal load current and $\tilde{i}_{\mathrm{load}}$ is the load current variation.

From (8), the dc bus voltage loop can be expressed by the following transfer function, written in the worst case (no load, which leads to a pure integrator behavior):

$$\left.\frac{\tilde{v}_{\mathrm{Bus_{Mea}}}(s)}{\tilde{v}_{\mathrm{Bus_{REF}}}(s)}\right|_{\mathrm{OL}} = \overbrace{G_V\frac{(T_{Vi}s+1)}{T_{Vi}s}}^{\text{PI Controller}} \cdot \overbrace{\frac{1}{CV_{\mathrm{Bus}}s}}^{\tilde{v}_{\mathrm{Bus}}(s)/\tilde{p}_{\mathrm{SuperC}}(s)} \cdot \overbrace{\frac{K_2}{T_{\mathrm{fv1}}s+1}}^{\text{filter}} \tag{9}$$

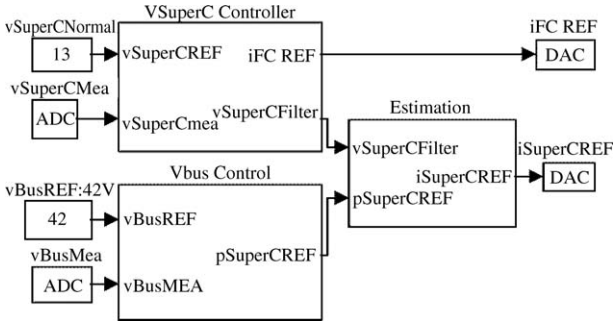

Fig. 6. Hybrid system context diagram.

3.3. Supercapacitor voltage loop

At last, to obtain the transfer function of the supercapacitor voltage loop, one can write the relationship of the powers as:

$$v_{\mathrm{FC}}(t)i_{\mathrm{FC}}(t) = v_{\mathrm{SuperC}}(t)i_{\mathrm{SuperC}}(t) + p_{\mathrm{load}}(t) \tag{10}$$

where v_{FC} is the fuel cell voltage, v_{SuperC} and i_{SuperC} are the supercapacitor voltage and current and p_{load} is the load power.

While considering that $v_{\mathrm{FC}}(t)$ and $p_{\mathrm{load}}(t)$ are disturbance of the system, Eq. (10) can be linearized under the form:

$$C_{\mathrm{SuperC}}\frac{\mathrm{d}\tilde{v}_{\mathrm{SuperC}}}{\mathrm{d}t} = \frac{V_{\mathrm{FC}}\tilde{i}_{\mathrm{FC}}}{V_{\mathrm{SuperC}}} \tag{11}$$

where V_{FC} is the nominal fuel cell voltage, V_{SuperC} is the nominal supercapacitor voltage, and $\tilde{v}_{\mathrm{SuperC}}$ is the supercapacitor voltage variation and C_{SuperC} is the supercapacitor capacitance.

Therefore, the supercapacitor voltage loop can be presented by the following transfer function:

$$\left.\frac{\tilde{v}_{\mathrm{SuperC_{Mea}}}(s)}{\tilde{v}_{\mathrm{SuperC_{REF}}}(s)}\right|_{\mathrm{OL}} = \overbrace{\frac{1}{T_i s}}^{I\text{Controller}} \times \overbrace{\frac{V_{\mathrm{FC}}/V_{\mathrm{SuperC}}}{C_{\mathrm{SuperC}}s}}^{\tilde{v}_{\mathrm{SuperC}}(s)/\tilde{i}_{\mathrm{FC}}(s)} \times \overbrace{\frac{K_3}{T_{\mathrm{fv2}}s+1}}^{\text{filter}} \tag{12}$$

4. Hybrid system implementation

Fig. 6 additionally depicts the realization for hybrid system algorithm in Matlab/Simulink environment for dSPACE interfacing card (real time card DS1104). The hybrid system communicates with the operator by means of ControlDesk software, and is linked with converters (acquisition of v_{SuperC} and v_{Bus}, generation of current reference signals $i_{\mathrm{SuperCREF}}$ and i_{FCREF}) by Digital to Analog Conversion (DAC) and Analog to Digital Conversion (ADC) of dSPACE interfacing card.

5. Experimental results and discussions

The hybrid test bench is presented in Fig. 7. The considered fuel cell is a 40 A, 500 W PEMFC stack, constructed by Zentrum für Sonnenenergie und Wasserstoff-Forschung (ZSW), Ulm, Germany, installed in a test bench provided by gas supply and control. Air is supplied from a compressor through a humidification unit, and pure dry hydrogen comes from bottles.

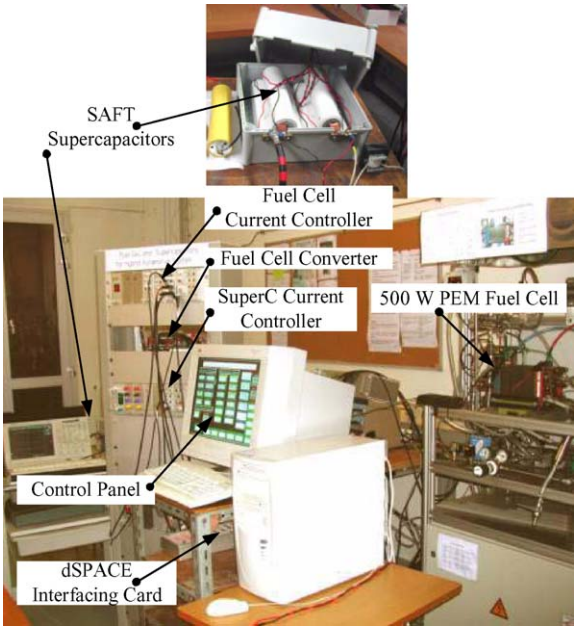

Fig. 7. Hybrid system test bench.

A cooling system permits to impose a constant stack temperature by heating or cooling of the water circuit. A programmable controlling unit contains all necessary control functions as reference setting, measurement conditioning, and security shutdown. The stack contains 23 cells with an active surface of 100 cm^2. The experiment is carried out under a stack temperature of 55 °C, a humidifier temperature of 45° [23]. Besides, its simplified diagram is illustrated in Fig. 8.

5.1. Fuel cell converter testing with a PEM fuel cell

In a practical system, when fuel cell operates, its fuel flow is controlled by fuel cell processor, which receives current demand from current reference as shown in Fig. 4. The fuel flow must be adjusted to match the reactant delivery rate to the usage rate.

Nonetheless, to present the fuel cell characteristics, this test bench is operated in two different ways for fuel flow. Firstly, fuel cell works at constant fuel flow corresponding to the maximum available current of 50 A (40 A is the rated current). In this case, the fuel cell has always enough hydrogen and oxygen. Secondly, the fuel flow varies depending on fuel cell current reference.

Figs. 9 and 10 present the dynamic response of fuel cell current loop to a step reference, in the case of constant fuel flow

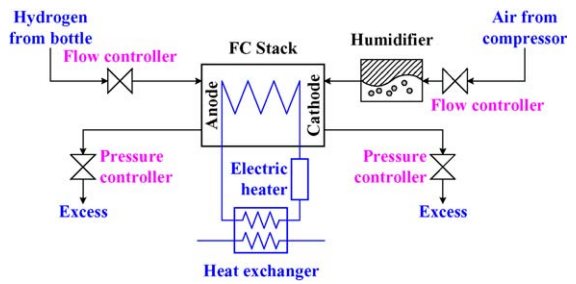

Fig. 8. Simplified diagram of the ZSW 500 W PEM fuel cell system.

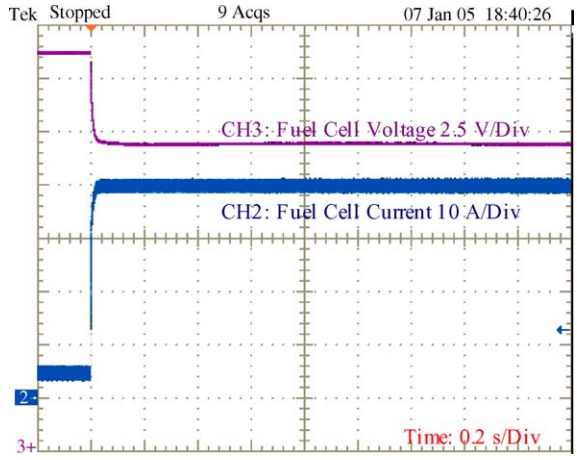

Fig. 9. Fuel cell current response to a 10–40 A step reference at constant fuel flow (set for 50 A).

for Fig. 9, and in the case of adjusted fuel flow for Fig. 10. One can observe on voltage curve in Fig. 10, compared with Fig. 9, the effect of mechanical delay which implies that fuel supply and delivered electrical current do not coincide. Fuel flow has difficulties to follow the current step, and this condition of operating is evidently hazardous for the fuel cell stack and will essentially lead to degrade the stack lifetime. It is essential to note that Schenck et al. [9] obtained the same kind of response, and similar time response, with a 1.2 kW Ballard fuel cell. Therefore, to utilize fuel cell in dynamic application, its current slope must be limited in order to insure a good synchronization between fuel flow and fuel cell current. In addition, the steady-state characteristics of the PEM fuel cell when connecting with converter, with switching frequency of 25 kHz, are also illustrated in Figs. 11 and 12. One can observe that the PEM fuel cell contains complicated impedance component [23].

5.2. Hybrid system test bench

Technical specifications of the test bench are as follows: $L_1 = 72\ \mu H$, $L_2 = 54\ \mu H$, $C = 0.702$ F. The supercapacitive stor-

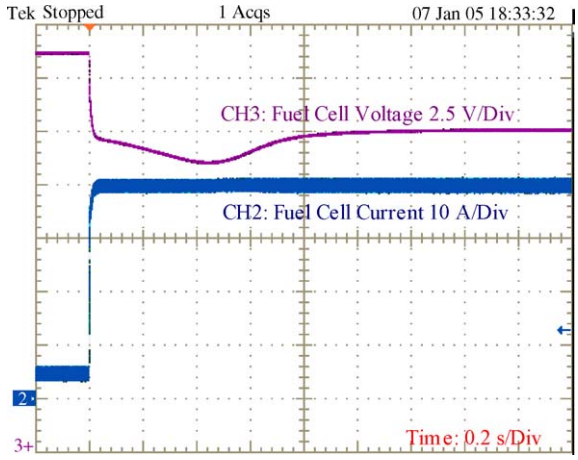

Fig. 10. Fuel cell current response to a 10–40 A step reference at variable fuel flow.

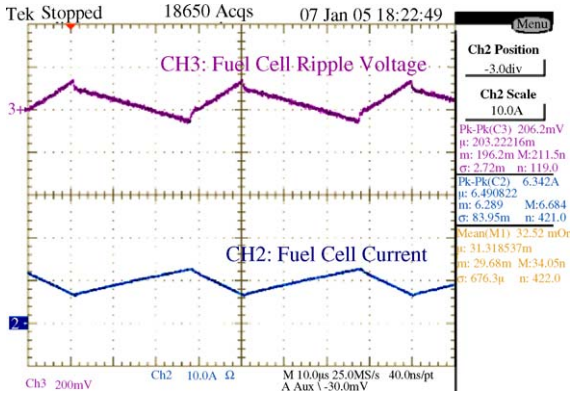

Fig. 11. Steady-state characteristics of the PEM fuel cell at 10 A.

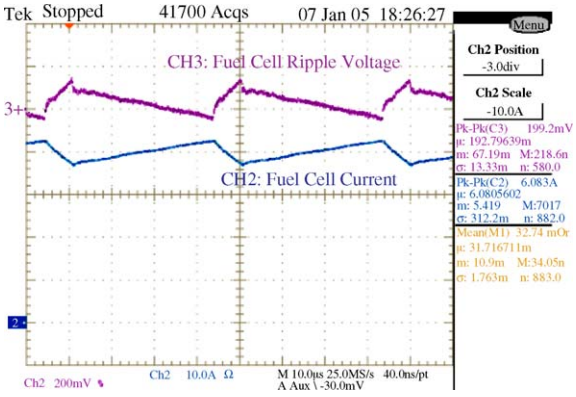

Fig. 12. Steady-state characteristics of the PEM fuel cell at 40 A (rated).

age device is obtained by means of six SAFT supercapacitors (3500 F, 2.5 V, 400 A, ESR: 0.8 mΩ) connected in series.

- The fuel cell current loop parameters are $D = 0.7$, $V_{\mathrm{Bus}} = 42$ V, $R_{L_1} = 10\,\mathrm{m\Omega}$, $V_{\mathrm{P}} = 10$ V, fuel cell current slope limitation set to $4\,\mathrm{A\,s^{-1}}$, $I_{\mathrm{FCRated}} = 40$ A, $I_{\mathrm{FCMin}} = 5$ A, $K_1 = 8$ V/40 A, $T_{\mathrm{fc}} = 1$ ms, $T_{\mathrm{Cd}} = 1$ ms, $T'_{\mathrm{Cd}} = 2\,\mu$s, $T_{\mathrm{Ci}} = 0.381$ ms and $G_C = 0.02$.
- The dc bus voltage loop parameters are $K_2 = 1$ V/1 V, $T_{\mathrm{fv1}} = 20$ ms, $T_{Vi} = 0.245$ s and $G_V = 800$.
- The supercapacitor voltage loop parameters are $\Delta v = 0.5$ V, $I_{\mathrm{SuperCRated}} = 200$ A, $V_{\mathrm{SuperCNormal}} = 13$ V, $V_{\mathrm{SuperCMax}} = 15$ V, $V_{\mathrm{SuperC}Min} = 8$ V, $K_3 = 1$ V/1 V, $T_{\mathrm{fv2}} = 0.16$ s and $T_i = 10$ ms.

Note that the rated power of the main source is 500 W, but system has some losses. Then, dc bus can absorb about 440 W from fuel cell power. This means that rated power at dc bus is 440 W. From now, the fuel flow is adapted to the value of the delivered current to improve the efficiency of the system.

The experimental tests presented hereafter have been carried out by connecting to the dc bus a resistance, and an active load composed of a current reversible chopper loaded by an inductance in series with two batteries. The current through batteries is controlled by means of a hysteresis corrector.

Fig. 13 presents hybrid characteristics during supercapacitor charge from 11 V to 13 V. At the beginning of charge (from $t = 1$ to 10 s), the fuel cell current reaches its rated value with a slope of $4\,\mathrm{A\,s^{-1}}$. At $t = 60$ s, v_{SuperC} is equal to 13 V, and then charging current is reduced. Because of the sloped limitation of fuel cell current, v_{SuperC} reaches over 13 V. As a result, system

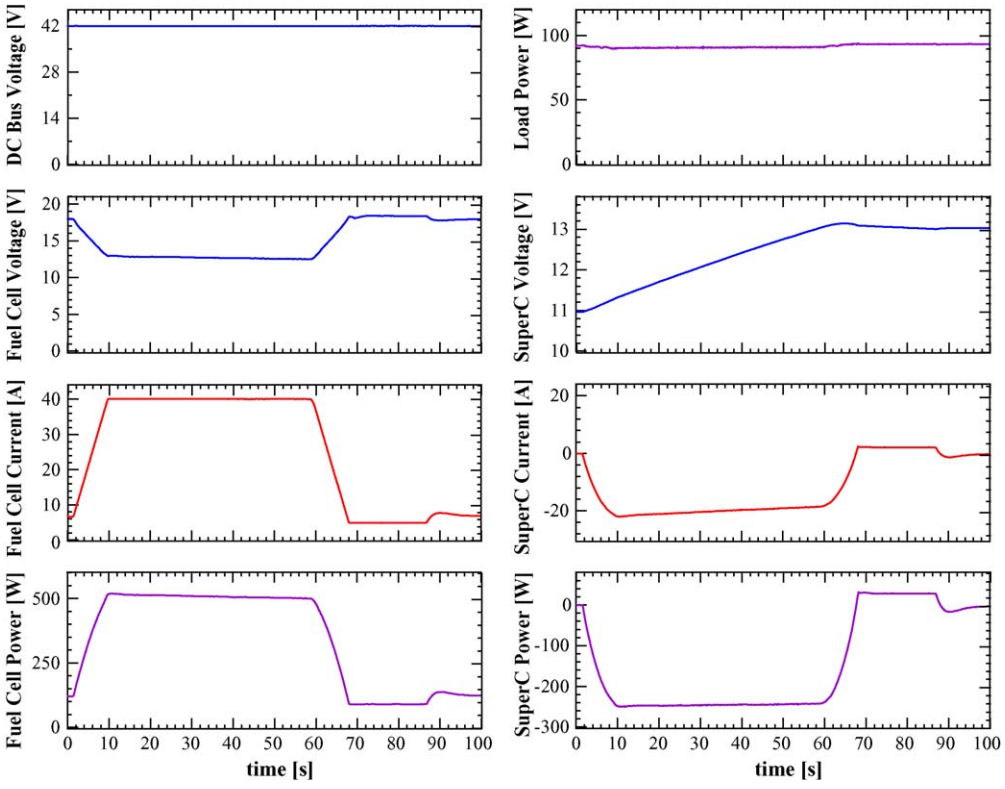

Fig. 13. Charging supercapacitors from 11 to 13 V.

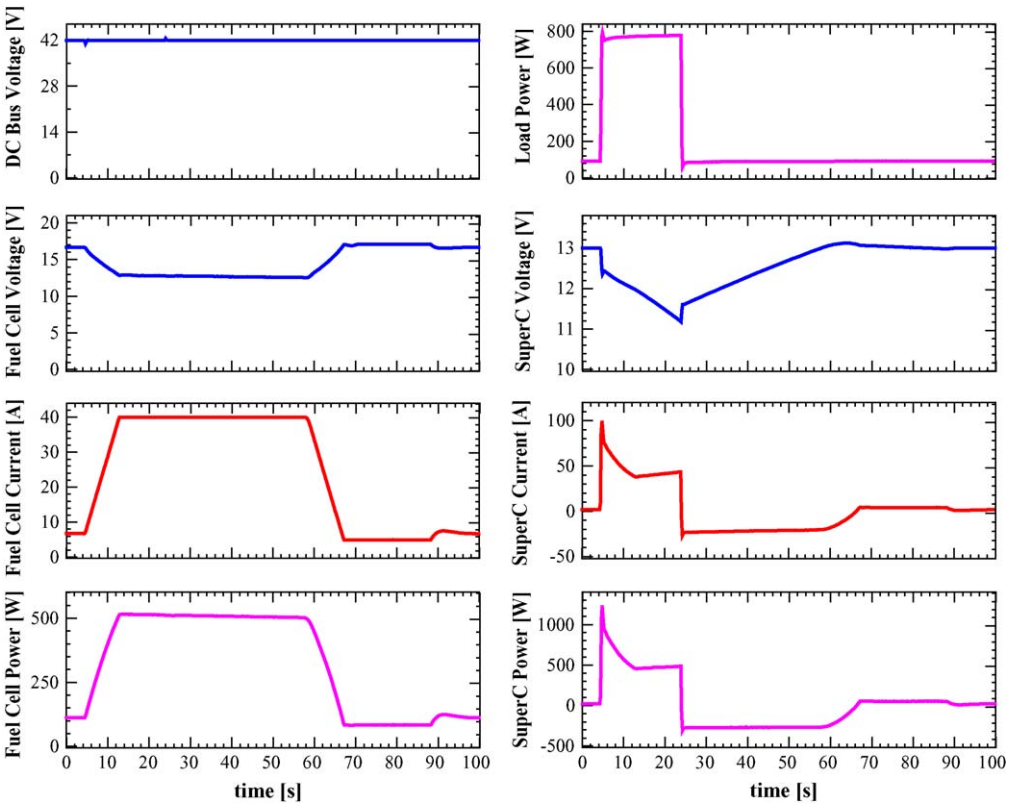

Fig. 14. Hybrid system response when overloading by 177%.

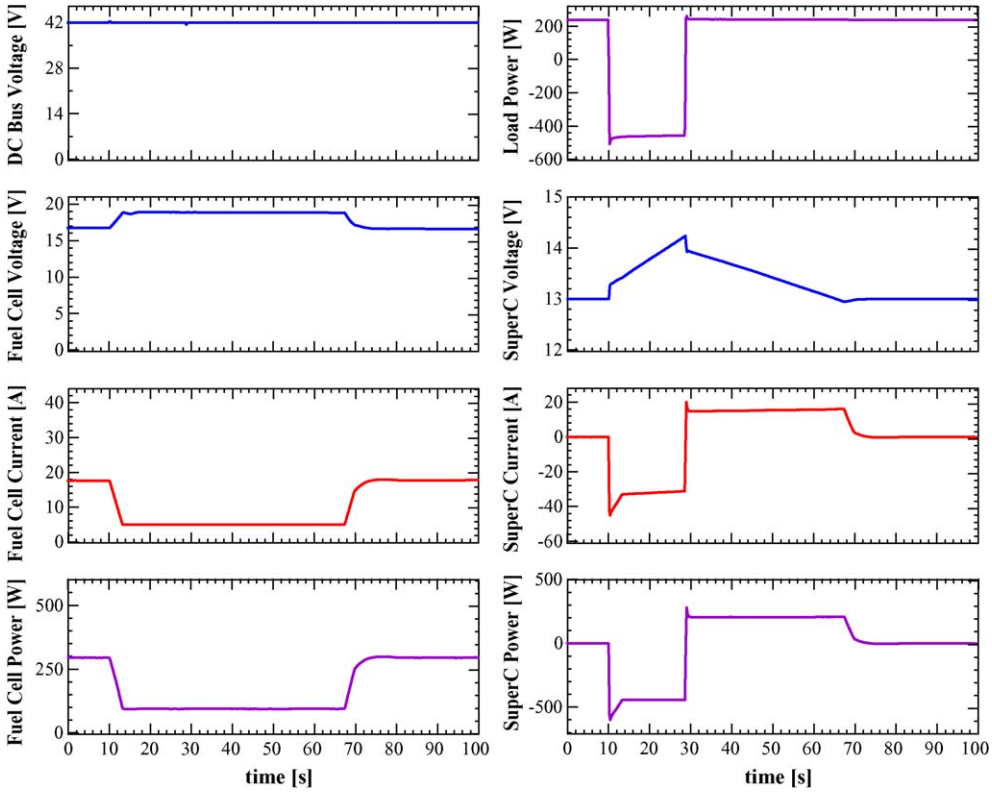

Fig. 15. Hybrid system response when recovering.

tries to discharge supercapacitors at $t = 68$ s. At the end of charge ($t = 96$ s), fuel cell current comes back to beginning value for constant load at dc bus, and i_{SuperC} comes back to nearly zero.

Fig. 14 presents transient responses of the hybrid system to an excessive load of 177% (created by the active load) during 20 s. It shows that the supercapacitors compensate the main source during both transient state and steady state. During the transient state, beginning at $t = 5$ s, the current delivered by the fuel cell slowly increases (with a controlled slope of $4\ A\ s^{-1}$) up to its rated value. During the steady state, beginning at $t = 12$ s, fuel cell current is equal to its rated value. In both cases, fuel cell power is not enough to supply the load power, and thus the dc bus voltage regulation leads supercapacitors to deliver the lacking energy. Then, the sudden decrease of the load power at $t = 24$ s gives rise to charge supercapacitors because v_{SuperC} is lower than $V_{SuperCNormal}$. Fuel cell current i_{FC} still stays at its rated value. Clearly, control system can excellently regulate the dc bus voltage, even though the high peak load. Furthermore, the fuel cell problems of fuel flow are noticeably avoided by controlling its current slope.

As a final test, Fig. 15 corresponds to a sudden recovery of energy on the dc bus from $t = 10$ s to 28 s. This energy is recovered by the supercapacitors, while fuel cell current slowly decreases ($-4\ A\ s^{-1}$) down to its minimum value. When the recovery period is finished at $t = 28$ s, i_{SuperC} changes in order to discharge the supercapacitors, because v_{SuperC} is over than $V_{SuperCNormal}$. Therefore, fuel cell current still keeps its minimum value until v_{SuperC} is equal to $V_{SuperCNormal}$. After that fuel cell current rises back to its initial value, to supply constant power load (about 240 W) at dc bus.

6. Conclusion

This work presents a new method of regulating dc bus for electric vehicle applications supplied by hybrid sources using a PEM fuel cell, as main power source, and supercapacitors as auxiliary power source. The essential constrain is to avoid rapid transition of fuel cell current in order to prevent fuel (hydrogen and oxygen) starvation problem by controlling fuel cell current slope, and then to reduce mechanical stresses on the system (fuel pressure, water pressure in tubes and stack). The control strategy is that dc bus voltage controller operates on a fast power source, supercapacitors, and the supercapacitor voltage being control by the fuel cell delivered current.

The experimental results on a small-scale dc bus (42 V, 500 W), with a 12.5 V, 500 W PEM fuel cell, have confirmed the fuel starvation phenomena. Results carried out by means of a hybrid system test bench, which employs a storage device composed of six SAFT 3500 F supercapacitors connected in series, have evidently revealed the excellent performances of the proposed control principle in conditions of overload and energy recovery in a short time.

References

[1] C.K. Dyer, Fuel cells for portable applications, J. Power Sources 106 (1–2) (2002) 31–34.
[2] B.D. McNicol, D.A.J. Rand, K.R. Williams, Fuel cells for road transportation purposes—yes or no? J. Power Sources 100 (1–2) (2001) 47–59.
[3] M.A.J. Cropper, S. Geiger, D.M. Jollie, Fuel cells: a survey of current developments, J. Power Sources 131 (1–2) (2004) 57–61.
[4] M.W. Ellis, M.R. Von Spakovsky, D.J. Nelson, Fuel cell systems: efficient, flexible energy conversion for the 21st century, Proc. IEEE 89 (12) (2001) 1808–1818.
[5] K. Chandler, B.L. Eudy, Thunder power bus evaluation at sun line transit agency, prepared for the DOE, Contract No. DOE/GO-102003-1786, November 2003 http://www.nrel.gov/docs/fy04osti/34379.pdf.
[6] P. Rodatz, G. Paganelli, A. Sciarretta, L. Guzzella, Optimal power management of an experimental fuel cell/supercapacitor-powered hybrid vehicle, Control Eng. Pract. 13 (1) (2005) 41–53.
[7] J.T. Pukrushpan, A.G. Stefanopoulou, H. Peng, Controlling fuel cell breathing, IEEE Control Syst. Magazine 24 (2) (2004) 30–46.
[8] J.T. Pukrushpan, A.G. Stefanopoulou, S. Varigonda, L.M. Pedersen, S. Ghosh, H. Peng, Control of natural gas catalytic partial oxidation for hydrogen generation in fuel cell applications, IEEE Trans. Control Syst. Tech. 13 (1) (2005) 1–14.
[9] M.E. Schenck, J.S. Lai, K. Stanton, Fuel cell and power conditioning system interactions, in: Proceedings of IEEE-APEC 2005, Texas, USA, 6–10 March, 2005, pp. 114–120.
[10] P. Thounthong, S. Raël, B. Davat, Test of a PEM fuel cell with low voltage static converter, J. Power Sources, http://authors.elsevier.com/sd/article/S03787753050 01564.
[11] J.M. Corrêa, F.A. Farret, L.N. Canha, M.G. Simões, An electrochemical-based fuel cell model suitable for electrical engineering automation approach, IEEE Trans. Ind. Electron 51 (5) (2004) 1103–1112.
[12] S.H. Choi, J. Kim, Y.S. Yoon, Fabrication and characterization of a $LiCoO_2$ battery–supercapacitor combination for a high-pulse power system, J. Power Sources 138 (1–2) (2004) 360–363.
[13] A. Burke, Ultracapacitors: why, how, and where is the technology, J. Power Sources 91 (1) (2000) 37–50.
[14] A. Rufer, D. Hotellier, P. Barrade, A supercapacitor-based energy-storage substation for voltage-compensation in weak transportation networks, IEEE Trans. Power Delivery 19 (2) (2004) 629–636.
[15] J.W. Dixon, M.E. Ortuzar, Ultracapacitors + dc–dc converters in regenerative braking system, IEEE Aerospace Electron. Syst. Magazine 17 (8) (2002) 16–21.
[16] E. Faggioli, P. Rena, V. Danel, X. Andrieu, R. Mallant, H. Kahlen, Supercapacitors for the energy management of electric vehicles, J. Power Sources 84 (2) (1999) 261–269.
[17] M. Ortúzar, J. Dixon, J. Moreno, Design construction and performance of a buck-boost converter for an ultracapacitor-based auxiliary energy system for electric vehicles, in: Proceedings of IEEE-IECON 2003, Roanoke, Virginia, USA, 2–6 November, 2003.
[18] A. Rufer, P. Barrade, A supercapacitor-based energy-storage system for elevators with soft commutated interface, IEEE Trans. Ind. Appl. 38 (5) (2002) 1151–1159.
[19] P. Thounthong, S. Raël, B. Davat, Supercapacitors as an energy storage for fuel cell automotive hybrid electrical system, Int. J. Electrical Eng. Transportation 1 (1) (2005) 21–25.
[20] P. Thounthong, S. Raël, B. Davat, Utilizing fuel cell and supercapacitors for automotive hybrid electrical system, in: Proceedings of IEEE-APEC 2005, Texas, USA, 6–10 March, 2005, pp. 90–96.
[21] R.D. Middlebrook, S. Cuk, A general unified approach to modeling switching-converter power stages, Int. J. Electron. 42 (6) (1977) 521–550.
[22] V. Vorperian, Simplified analysis of PWM converters using model of PWM switch—continuous conduction mode, IEEE Trans. Aerospace Electron. Syst. 26 (3) (1990) 490–496.
[23] W. Friede, S. Raël, B. Davat, Mathematical model and characterization of the transient behavior of a PEM fuel cell, IEEE Trans. Power Electron. 19 (5) (2004) 1234–1241.